NRC Canada Work on Inspection of Weak Bonds – An Overview

Richard G. Cole[1], James M. Sands[2], Christophe Bescond[3], Daniel Lévesque[3]
CANADA

[1] NRC Aerospace Research Centre, Ottawa, Canada
[2] United States Army Research Laboratory, Aberdeen Proving Grounds, Maryland, USA (on sabbatical with NRC Aerospace, Ottawa, Canada during this work)
[3] NRC Energy, Mining, and Environment Research Centre, Boucherville, Canada

Rick.Cole@nrc-cnrc.gc.ca

ABSTRACT

Over the past decade, the National Research Council of Canada (NRC) has been conducting research to develop technologies that will help users to find weak adhesive bonds. In general, adhesive bonding is not permitted for construction of flight-critical aircraft structures because there is no Non-Destructive Inspection (NDI) technique that can provide confidence in the quality of bonded joints. NRC's work has focussed on two areas: development of methods to reliably create weak adhesive bond specimens, and development of NDI methods to inspect bond strength. This paper summarizes NRC's efforts to control the reactivity of adhesives and adherends during bonding in order to create controlled bond strength specimens, as well as efforts to develop the laser shock technique as a means of interrogating the through-thickness tensile strength of adhesive bonds. Technical feasibility has been proven for NRC's approaches in both of these areas.

1.0 INTRODUCTION

The application of fibre-reinforced polymer composites to improve the performance of aircraft structures is well established. However, in many applications structures could be further optimized and design weights reduced if it were possible to use adhesive bonding in place of mechanical fasteners in structural assembly. Unfortunately, regulatory requirements and their typical application in aircraft certification and qualification programs generally do not allow highly loaded adhesively bonded joints without the aid of fasteners, particularly when the bonded joints must carry primary flight loads. This major limitation is principally due to the lack of Non-Destructive Inspection (NDI) techniques that can validate bond strength and integrity [1].

NRC Canada has been working for some years on the development of advanced NDI techniques that can detect poor quality bonds. One of the keys to successful validation of advanced NDI techniques is the ability to manufacture bonded specimens with controlled joint strength. While high-strength adhesive bonds are reasonably well understood and can be achieved through careful process controls, the creation of weakly bonded joints with controlled reduced-strengths is not well known. The methodologies presented here to create controlled bond strength were initially trialled on metallic substrates and then extended to composite substrates. Two approaches were developed to control bond strength. First, the interface of the metallic substrates was modified by treatment with a custom formulated primer based on functional silane coupling agents. These coupling agents bond strongly to the substrate surface but can be selected to have varying degrees of reactivity with the adhesive. Mixtures of coupling silanes have been demonstrated to be effective tether materials to surfaces by many researchers [2-5]. By control of the silane mixture, the resulting bond can be controlled to be weaker than the optimum bond strength of the adhesive. The custom bond primer method is easily applied to metallic substrates that form metal-oxide layers and can be used with any form of adhesive (i.e. film or paste). To expand this technique to composites, it is necessary to apply a thin metallic layer on the substrate surface prior to application of the primer. The second approach used to control bond strength was to reformulate an aerospace-grade two-part paste adhesive to control

the chemical reaction and degree of chemical conversion by reducing hardener content, with the novel innovation of balancing the reduction in crosslinking monomers by including an additional component to convert 100% of reactive epoxy bonds in the adhesive. The resulting adhesive has property stability with time (compared to a partially reacted adhesive system), while having limited ability to form coupling interactions between the adhesive and substrate. Though this approach is only effective for two component paste adhesives, the modification can be applied to any substrate and on any primer treatment. The following paper summarizes the work performed at NRC to develop systematic methods of creating controlled-strength adhesive bond specimens that can be used for developing advanced NDI technologies. Further details on this work are available in References [6] and [7].

Although there have been many attempts to develop NDI approaches for adhesive bonds, none of them has succeeded in detecting a weak bond other than those that are weakened by defects such as disbonds or porosity [8 - 10]. Ultrasonic techniques only apply weak stresses to the bond line and such weak stresses cannot reveal characteristics that only become apparent through significant stresses, such as in destructive tests. A convenient approach for evaluating the adhesion of coatings to substrates and matrices to fibres uses a pulsed laser to generate a large amplitude wave (shockwave) that propagates through the material [11 - 15]. This wave, being initially in compression, is converted by reflection on the back surface of the sample, into a strong tensile wave that can pry apart the sample and disbond the assembly. This approach has been recently extended to proof testing of adhesive bonds between carbon-epoxy laminates [16, 17]. To probe bond strength, higher and higher tensile stress loading is applied by increasing the laser pulse energy step by step. A "good" joint will be unaffected by a given stress level whereas a weak one will be debonded, allowing this method to evaluate bond strength. The following paper summarizes NRC's work on development of the laser shock technique for testing adhesive bonds. Further details are available in Reference [17].

2.0 CONTROL OF BOND STRENGTH

2.1 Control of Bond Strength Using Customized Surface Treatment

The objective of surface preparation in adhesive bonding has traditionally been to maximize the level of adhesion at the adhesive/substrate interface and to preserve that performance over broad thermal and environmental loading conditions [18]. For metallic substrates, researchers have demonstrated the critical value of coupling agents on bond durability [19]. These coupling agents act as a bridge, interacting covalently with the chemistry of both interfaces [20]. The most common coupling agent (i.e. bond primer) used for aluminum and other oxide-forming metals is silane, which is shown below in Equation 1:

$$R\text{-}CH_2\text{-}Si\text{-}(OCH_3)_3 \quad (1)$$

In the present research, the method of tuning bond chemistry involved maintaining the existing strong silane coupling adhesion to the metallic surface but varying the coupling efficiency with the adhesive through selection of reactive and non-reactive "R" groups. The intent was to weaken the interface between the coupling agent and the adhesive by reducing the proportion of silane reactive sites available for coupling to the reactive epoxies in the adhesive.

The concept for controlling interfacial strength of adhesives was derived from previous research involving the use of varying mix ratios of hydrolyzed 3-glycidoxypropyltrimethoxysilane (γ-GPS) and N-propyltrimethoxysilane (PTMO) to control coupling strength between a matrix resin and the surface of the fibres in a composite [21]. The mix ratios were tested over a broad chemical range and the results demonstrated that approximately 30% concentration of γ-GPS was sufficient to achieve maximum interfacial shear strength. Publications related to the application of these concepts on adhesive bonding specimens have been limited, though some results were presented to the authors by Dr. Steven H. McKnight (formerly of United States Army Research Laboratory) [22].

Details on preparation of the mixtures used in the research described herein are contained in References [6] and [7].

2.2 Control of Bond Strength by Chemical Reformulation of Paste Adhesive

The concept of controlling adhesion strength in two-part adhesives by modifying mix ratios is not new, however this approach usually results in significant changes in the mechanical properties of the adhesive, including long term stability and performance, by leaving unreacted functional groups that pick up uncontrolled constituents such as moisture from the environment over time [23]. For the purposes of the present study it was desired to stabilize the bond properties by completely consuming the functional groups in the adhesive.

Loctite's Hysol EA9394 two-part aerospace epoxy-amine adhesive was the paste adhesive selected for this work. The ideal mix ratio of Part A to Part B is 100:17. Mixing on-stoichiometry and curing according to the adhesive supplier's datasheet results in optimum (100%) strength bonds [24]. For this two-part epoxy paste adhesive, Part A is the epoxy resin and Part B is the amine hardener. To terminate cross-linking and acquire stability in the system, a terminating amine, cyclohexylamine (CHA), was selected and added stoichometrically to react and fully convert the functional epoxy groups. This third component is referred to herein as Part C, and was selected to provide end-capping and linear polymer chain formation in the adhesive. Fourier Transform Infrared Spectroscopy (FTIR) was used to investigate and measure the concentration of un-reacted epoxy in off-stoichiometric blends in order to determine the optimal concentration of Part C to completely react the epoxy in the system. Details on the measurement method are included in Reference [6].

2.3 Bond Strength Control Process Development Trials – Aluminum Specimens

The adhesives selected for the present study were Cytec Corporation's FM73 film adhesive and Loctite Corporation's Hysol EA9394 paste adhesive. To develop the different bond strength-control processes, the Single Lap Shear (SLS) test method with aluminium adherends as defined in ASTM D1002 [25] was used. Although this test induces both shear and peel loads in the bondline, which may have introduced a degree of variability in the results [26], it was selected as a simple and quick method to generate comparative test results between the full strength and weak bonded specimens. Aerospace grade aluminum (2024-T3, 1.6 mm thick) was selected as the substrate due to its common use in aerospace structures and the availability of substantial surface treatment and adhesive strength data for this material.

The aluminum panels were prepared for bonding using a standard surface preparation method including grit-blast and cleaning using a blast of dry nitrogen and wiping with methyl ethyl ketone (MEK). After a thin layer of native oxide reformed on the surface, primer was applied to prepare the interfacial region for bonding. For those panels involved in the customized surface treatment approach, custom silane treatments were applied. For those panels intended for use in the reformulated paste adhesive approach, a high bond strength silane surface treatment of 100% γ-GPS was applied. After treatment, the aluminum substrates were bonded using either FM73 or EA9394 to produce specimens for mechanical testing. FM73 was cured at 121°C ± 3°C for one hour using an autoclave according to the adhesive supplier's recommended process [27]. EA9394 was cured at room temperature for 24 hours and then underwent accelerated curing at 66°C ± 3°C for one hour following the adhesive supplier's recommended process [24]. SLS specimens were cut from the bonded panels to meet the dimensions of ASTM D1002. Average bondline thickness for specimens prepared with FM73 ranged from 0.15 mm to 0.30 mm. For EA9394, the bondline thickness ranged from 0.13 mm to 0.25 mm.

SLS specimens were tested in accordance with ASTM D1002 on an Instron 1125 load frame, using mechanical wedge grips, at room temperature ambient conditions. The loading rate was 1.3 mm/minute under displacement control and loading was continued until failure. Figure 1 shows the test set up and coupon configuration.

Figure 1 : SLS test set up and coupon configuration

2.3.1 Aluminum Specimens – Bond Strength Results

Customized Surface Treatment:

By tuning the interfacial chemistry at the primer-adhesive layer, different strengths of adhesive bonds were successfully obtained. Figure 2 shows the effect that increasing the proportion of the weak coupling surface treatment (PTMO) had on reducing bond strength. The critical level of PTMO where bond strength was dramatically reduced is clearly shown for both FM73 and EA9394. In the plot of SLS strength versus proportion of PTMO, the critical level was different for the two adhesives. The drop in adhesion strength occurred with a proportion of approximately 15% of γ-GPS (85% PTMO) for FM73, and approximately 25% of γ-GPS (75% PTMO) for EA9394.

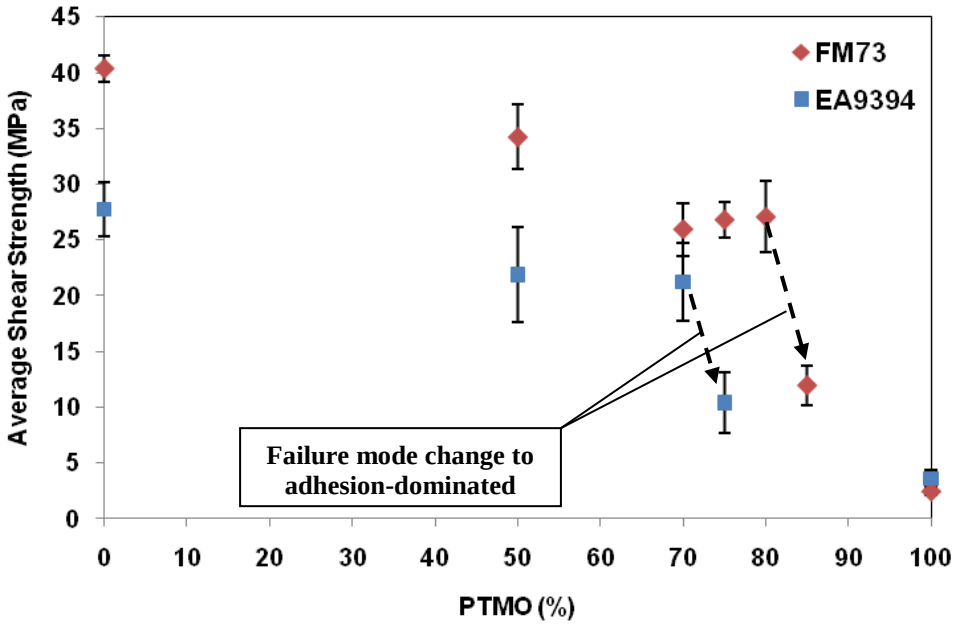

Figure 2 : Single Lap Shear strength versus PTMO proportion for weak bonds created by tuning chemistry using γ-GPS and PTMO for FM73 and EA9394 (error bars represent one standard deviation)

Close examination of the failed specimens noted a clear transition in failure mode at the critical threshold. For both adhesive types, specimens failed in either fully cohesion or mixed cohesion-adhesion modes below the critical proportion, while they very clearly failed in mixed adhesion-cohesion or fully adhesion mode at PTMO proportions above the critical level. Based on the previously cited research [21, 22] and on consideration of the clear change in failure mode, these results are consistent with a weakened silane/adhesive interface caused by selective coupling between the silane primer and the adhesive.

Reformulated Paste Adhesive:

By reducing the proportion of hardener (Part B) when mixing EA9394 paste adhesive, different strengths of adhesive bonds were successfully obtained. As discussed above, a terminating amine (Part C) was also included in order to return the mixture to stoichiometric balance. According to the adhesive supplier's instructions, the optimal mix ratio of Parts A and B is 100:17. FTIR analysis determined that reasonably high proportions of Part C were required to rebalance stoichiometry: a mixture with 3 parts of B required 11 of C, while a mixture with no B required 30 parts of C. Figure 3 shows the resulting strengths that were measured using the ASTM D1002 Single Lap Shear test.

It was noted that the inclusion of Part C gave the adhesive higher stiffness than the supplier's recommended A:B mixture. To investigate this effect, some mixtures were tested with and without Part C. Figure 3 shows both the partially reacted off-stoichiometry A:B adhesives and the fully terminated A:B:C adhesive formulations. As can be seen, a ratio of 100:3:11 showed retention of only 25% of the optimum bond strength, with an almost 50% reduction in strength over the 100:3 A:B mixture. The loss of strength with the addition of Part C is likely attributable to the previously noted increase in adhesive stiffness, and therefore reduced strain capacity, of the A:B:C formulations. As adhesive stiffness increases, the ability to deform under applied load is reduced, putting

more emphasis on coupling efficiency between the adhesive and the substrate surface, particularly in peel. As previously discussed, the ASTM D1002 test induces significant levels of peel load in the adhesive bond.

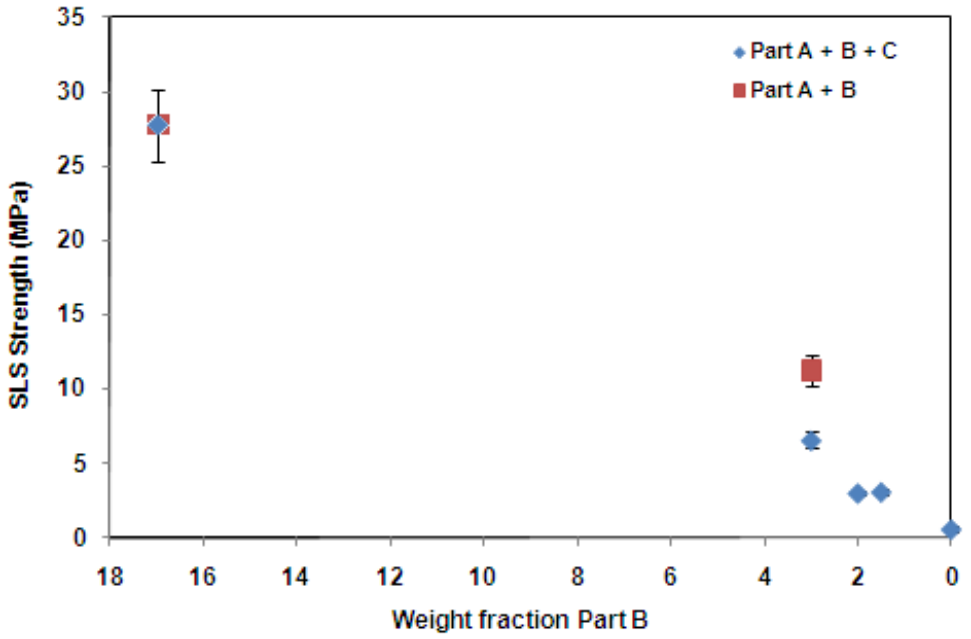

Figure 3 : Single Lap Shear strength versus Parts of B for chemically modified EA9394 system (error bars represent one standard deviation)

From a detailed review of the tested specimens, it was observed that with reduced strength, the specimen failures transitioned from cohesion-dominated to adhesion-dominated. It is considered that a principal reason for this transition was the increase in adhesive stiffness and the resulting decrease in strain capacity, particularly with regard to peel stresses.

2.4 Bond Strength Control – Composite Specimens

For this study, quasi-isotropic panels were manufactured by hand layup and autoclave curing of Cytec CYCOM 5276-1 unidirectional carbon fibre prepreg. Composite panels of 4 and 8 ply thickness were prepared using a $[-45/0/45/90]_{ns}$ lay-up sequence.

Although the reformulated paste adhesive approach allowed adhesive bonding of composite panels using conventional surface preparation techniques, the customized surface treatment approach required a strong, stable metal-oxide surface layer to anchor the custom silane mixture. To enable this, the composite panels were plasma cleaned and a PVD process was used to apply a thin layer of titanium to the laminate surface. Plasma cleaning was performed using an Advanced Energy (AE) RFX 600 13.56 MHz RF power supply with ultra-high purity Argon at a pressure of 7 mT as the working gas. The metal film was deposited using an Angstrom Sciences Onyx 3 inch magnetron sputtering gun driven by an AE MDX 500 power supply. This provided a nominal titanium film thickness of 0.10 microns, which was selected as sufficient for silane bonding purposes yet thin enough to not interfere with the laser shock bond test method. Further details of the metallizing process are provided in Reference [7]. Surface preparation and bonding of the composite test panels followed the same processes as described above for the aluminium specimens.

2.4.1 Composite Specimens – Bond Strength Results

The Double Cantilever Beam (DCB) test defined in ASTM D5528 [28] was selected for testing the bond strength of the composite specimens since this test applies a through-thickness tensile load to the bond in a manner more representative of the laser shock loading than the in-plane shear plus peel load applied during the single lap shear test. Testing was performed on an MTS Table Top 828 load frame, at room temperature ambient conditions. Figure 4 shows the test set up and coupon configuration. The loading rate was 1.5 mm/minute under displacement control and loading was continued until the crack propagated at least 38 mm from the PTFE film insert crack-starter.

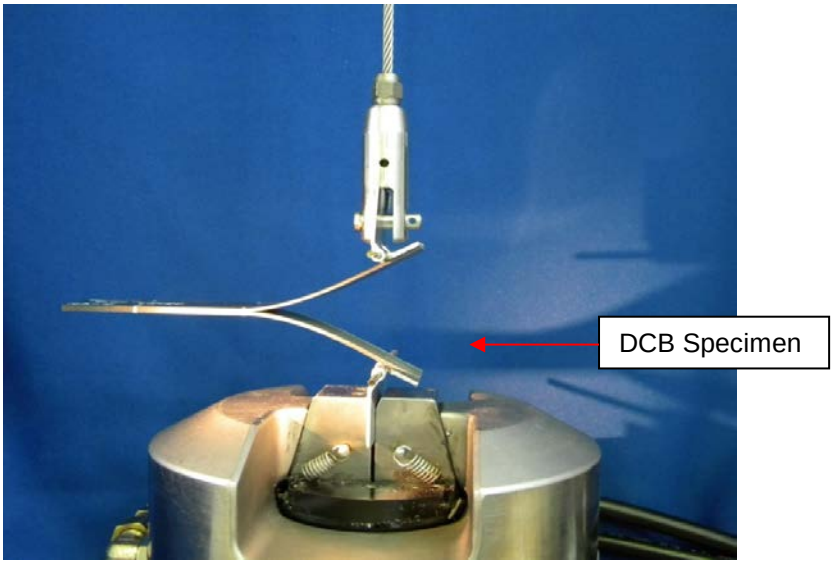

Figure 4 : DCB test set up and specimen configuration

Unfortunately, fewer specimens were available for DCB testing than had been used during the SLS tests. While the DCB test results followed the same general trends of bond strength versus primer mixture or paste adhesive mixture as were found during the SLS tests, for some bond types DCB data variability was much higher. DCB test Coefficients of Variation (CV ; standard deviation divided by mean value) of 8 to 26% were found, with the weaker bonds providing the higher CVs. Inspection of the failure surfaces of the customized surface treatment specimens indicated that the metallic layer remained in place and was not disbonded during testing. This provides confidence in the technique used to metalize the composite panels and suggests that it was not a contributing factor to the high CVs. Available specimens and time did not permit detailed investigation of the cause for this variability, and this work remains to be done.

3.0 LASER SHOCK EVALUATION OF BOND STRENGTH

3.1 Principle of the Approach

The laser shock evaluation approach is illustrated by the sketch shown in Figure 5. Real-time monitoring is provided by a laser interferometer that measures the back surface velocity. The signal from the interferometer allows the method to identify whether the bond has been broken or not. It also allows quantitative evaluation of the bond strength at the high tensile rate produced by the technique. The method is briefly reviewed here with more details found in Reference [17].

The laser shock generated wave is essentially a compression wave propagating normal to the surface. Figure 6 shows the propagation distance-time diagram for the evolution of a compression wave generated at the top sample surface with a loading time duration T and reflected by the free back surface as a tensile wave. In the small triangle with baseline delimited by the times t_1 and t_2 on the back surface, the incoming compression wave is essentially compensated by the reflected tensile wave. For a typical shock pulse shape, the maximum tensile stress (represented as a white circle) begins at a distance from the back surface given by DT/2, and this tensile wave propagates unchanged until the next reflection. Here, D is the shock wave propagation velocity which, in the conditions used, is essentially constant and close to the elastic wave propagation velocity c since the pressure level is significantly below the Hugoniot Elastic Limit. Figure 6 therefore shows that there is a "dead zone" near the back surface of the sample. For the 4-ply composite schematically represented in Figure 6, this zone extends to the top of the bottom ply assuming a loading duration of about 100 ns and a ply thickness of about 150 µm (D ≈ 3000 m/s).

The pressure *P(z,t)* at any instant t and at a depth z from the back surface inside the plate is equal to the sum of the pressures produced by the wave propagating in the positive z direction and the one propagating in the negative z direction. Under the assumptions of one-dimensional propagation in a homogeneous material and no attenuation, the pressure can be expressed in terms of the back surface velocity signal *u(0,t)* as:

$$P(z,t) = \frac{1}{2}\rho D\left(u\left(0,t+\left|z/D\right|\right) - u\left(0,t-\left|z/D\right|\right)\right) \tag{2}$$

where ρ is the density and the factor 1/2 comes from the total reflection of the wave at the free surface. It is noted that this expression neglects possible reflections from the interface between the composite and the adhesive, and therefore assumes similar impedance values. More general expressions for the pressure at the top and bottom interface of the adhesive can be found in Reference [29]. As shown by experiments at NRC with different laser shock loadings below rupture, the velocity signals are essentially superimposed after normalization. This means that propagation is in the elastic regime, no plastic deformation occurs, and non-linear effects are very weak. A difference only occurs for loading cases above the disbond threshold. In this case the tensile wave is reflected by the opened interface as a compression wave, which gives in turn a positive increase in velocity measured on the back surface, i.e. an increase of the out-of-plane motion of this surface.

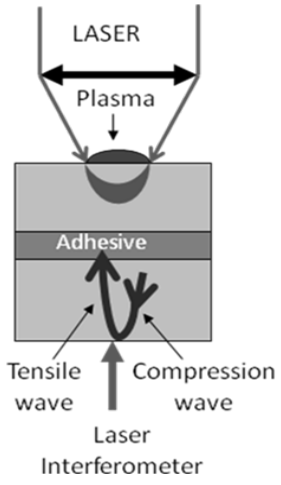

Figure 5 : Principle of the laser shockwave technique for probing an adhesive joint. The wave which is initially in compression is reflected by the free back surface as a tensile wave that performs tensile proof testing of the joint.

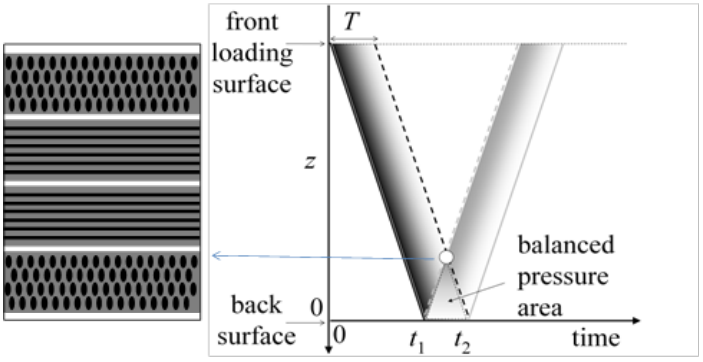

Figure 6 : Time-space diagram of the propagation of a shockwave pulse of duration T and schematic representation of the cross-section of a 4-ply composite laminate. Dark and light grey areas represent respectively the compression wave and tensile wave.

3.2 Implementation

To produce a strong compression wave, laser pulse generation in the ablation regime with plasma confinement is used. To maximize the pressure in the sample, a confining material with large acoustic impedance is required. This material has to be transparent to the laser light. Although confinement with a glass window produces a strong shockwave, the window is broken by each laser shot, so confinement with water is used, as shown in Figure 7. Since it would be unacceptable in practice to damage the surface of the material, common black electrical tape is placed on the surface. A Q-switched Nd:YAG laser operating at 1.06 μm and delivering a pulse of about 8 ns duration and 2 J energy has been used to date. As has been shown by measuring the velocity at the back of a transparent block of epoxy subjected to the same loading configuration, the protective tape has the effect of increasing the duration of loading [17]. This duration is on the order of 100 ns, rather than the value of approximately twice the laser pulse duration that has been shown by other researchers [30]. Since high frequencies are cut-off in composites by damping and scattering mechanisms, this longer loading duration is beneficial for maintaining the tensile stress level over a longer propagation distance.

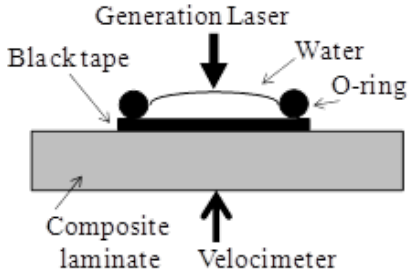

Figure 7 : Experimental setup for strong compression wave generation ensuring protection of the sample surface.

As discussed above, the stress applied throughout the sample can be determined from measurement of back surface velocity. This velocity is determined from the Doppler frequency shift produced on a light beam reflected by the surface. The light frequency change $\Delta\nu$ is proportional to the change of velocity Δu as follows:

$$\Delta\nu = 2\Delta u/\lambda \tag{3}$$

where λ is the laser wavelength. With the laser wavelength being 1.06 µm, a change of velocity of 100 m/s gives a frequency shift of about 100 MHz tracked by the interferometer. Although for shock experiments time-delay two-wave interferometers known as VISAR are traditionally used as velocimeter [31], we have developed one that is intrinsically simpler and makes use of the detection laser used for post-shock validation. It uses a solid Fabry-Perot etalon (FPE) [32]. The principle is similar to the use of a Fabry-Perot interferometer in optical spectroscopy where the spectrum of the source showing resonance peaks is obtained by scanning the path difference. Here, to use the FPE as a velocimeter, the frequency of the source is actually changing with time, due to the Doppler effect produced by the surface motion, the Fabry-Perot having a fixed thickness. Also, the frequency of the probing laser is set somewhere along the slope of a peak in the intensity versus frequency response. Since by the Doppler effect a change of frequency proportional to the surface velocity is produced, this results in an output from the detector after the FPE of an intensity signal indicative of the surface velocity, as illustrated in Figure 8. The output signal is only proportional to velocity if the linear portion of a peak slope is used. If this is not the case, the response has to be calibrated by recording the peak shape versus frequency. Actually, the peak shape is dependent upon the opening of the aperture after the FPE, i.e. it depends on the angular tilt of the optical waves propagating inside the FPE. Having a very limited angular range around zero, i.e. a very small aperture yields poor sensitivity since little light is collected, so the diaphragm aperture has to be opened to some extent.

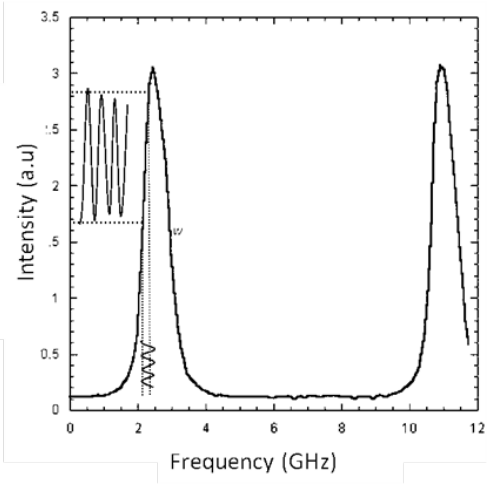

Figure 8 : Frequency demodulation with a Fabry-Perot etalon. The optical frequency of the probing laser is tuned to somewhere along a resonance peak to provide demodulation.

To get a reliable calibration curve that allowed translation of the recorded signal into a velocity signal, the voltage which controls the frequency sweep had to be calibrated in terms of frequency change. This was done by using an optical Michelson-type fibre interferometer with arms of very different lengths. By counting the fringes that appeared during frequency sweeps, precise calibration was obtained. The final calibration curve relates the normalized signal (signal measured by the detector after the FPE divided by a signal measured by another detector before the FPE) to the change in frequency and then velocity using Equation 3. As shown in Figure 9 by a black circle, after calibration by frequency sweeping, an initial frequency set point was chosen to provide good sensitivity to surface velocity, as well as ensuring a proper dynamic range for the velocities encountered in the experiments. Also, since a given signal amplitude can be associated with two frequency shifts or velocities, it was important to avoid going over the peak of the response for the maximum velocity to be measured, in order to avoid ambiguity. The usable range of velocity change is shown in Figure 9 by a heavy line with a dynamic range of about 200 m/s. The laser frequency was then locked to the set point with a feedback loop acting on the frequency controller for

the laser. This ensured that thermal drifts of the laser frequency or of the FPE resonance frequency were automatically compensated. The FPE was mounted with its associated optics in a rigid structure that was itself located in a rack. The detection beam, which came from a long-pulse single frequency Nd:YAG laser was projected onto the back surface of the sample using an optical fibre. Light reflected by the surface that carried information on its velocity during shockwave loading was also fibre -coupled to the FPE unit.

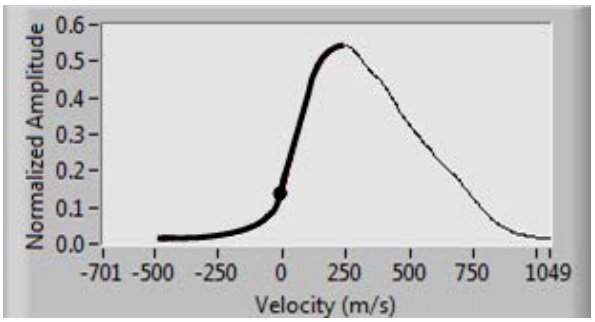

Figure 9 : Calibration curve of the velocimeter. The change of velocity at any time can be deduced from the measured normalized signal by using this curve. The dot indicates the initial set point.

Post-shock validation by ultrasonic inspection is necessary to validate any indications of rupture given by the real-time velocimeter, since this indication is often difficult to identify when loading is just above threshold. Ultrasonic inspection using the pulse-echo time of arrival technique provided the location of the disbond, which was necessary to evaluate bond strength. This inspection was performed with a laser-ultrasonic system that used the same kind of detection laser used for the velocimeter [33]. The generation laser was a Transversely Excited Atmospheric Pressure CO2 laser (TEA-CO2), as generally used for composite inspection. This laser has a wavelength within the absorption bands of the surface resin, epoxy or another polymer matrix, and from the through-depth distributed absorption, ensures efficient generation without damage to the material. Post-shock laser-ultrasonic inspection could be done from the loading surface, after the protective tape was removed, to produce short pulse and increase resolution for imaging the interfaces, or from the back surface.

3.3 Test results on composite specimens

In preliminary work, the laser shock technique was demonstrated with bonded quasi-isotropic carbon-epoxy laminates prepared with two areas of different adhesion strength. One area of each laminate was simply solvent cleaned, whereas the adjacent area was corona discharge activated to promote higher adhesion strength. Hysol EA9394 adhesive was used. As expected, very different adhesion strengths were measured, typically 150 MPa and 340 MPa [17]. It should be noted that due to the laser shock wave amplitude and frequency, these strengths were measured at very high strain-rates and therefore are higher than typical quasi-static values. Velocimeter indications of disbonding were found to correlate well with post-shock laser-ultrasonic inspection results.

To date, only some of the weak bond specimens created by the work described in Section 2 have been laser shock tested. Presented below are example results obtained on a specimen bonded with EA9394 and the customized surface treatment. The bond made to the metallized adherend had about 43% of the maximum strength (with variation of less than 5% between different samples when measured by DCB). The other adherend was not modified and had 100% bond strength. Like all samples, prior to laser shockwave loading the sample was inspected by digital x-ray radiography to check for porosity in the composite or bond line, and by laser ultrasonics to check for porosity and pre-existing delamination or disbond. This inspection ensured the laser shockwave testing could be performed over a defect-free area having only weak adhesion properties.

Figure 10 shows the back surface velocimeter signals obtained from this test specimen after normalisation of the signals for different loadings. As described above, disbonding was identified by the appearance of a significant offset after signal normalization. This occurred clearly for energy above 500 mJ energy loading. Figure 11 shows the confirmation of disbonding by laser-ultrasonic inspection. Using Equation 2 and the velocimeter signal at 458 mJ (below disbond), the bond strength of this sample was evaluated to be about 210 MPa in the high strain rate regime of the experiment.

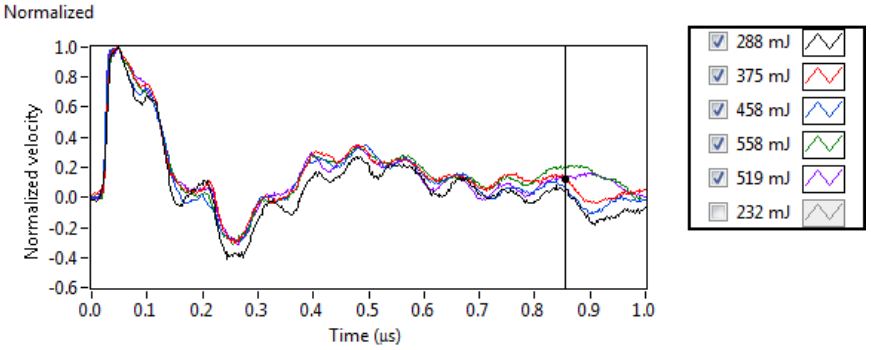

Figure 10 : Velocimeter signals obtained for a bonded 8-ply over 8-ply stack for different laser energy loadings, below and above damage threshold. The various signals have been normalized and the time of indication of rupture is shown by a vertical line.

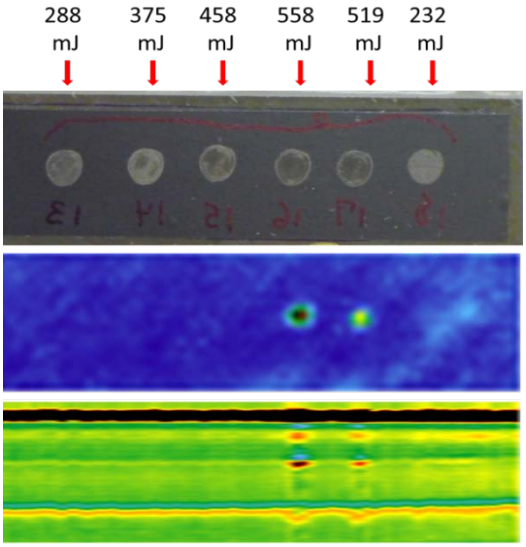

Figure 11 : Photo (top), laser-ultrasonic C-scan (sub-surface view, middle) and B-scan (cross-section view, bottom) for various laser energies. Disbond starts to be detected above 500 mJ energy loading.

4.0 CONCLUSIONS

Two techniques to reliably create weak adhesive bonds were demonstrated: customized surface treatments, and reformulation of paste adhesives. Single Lap Shear testing showed the abilities of both methods to create a wide range of bond strengths. Through-thickness tensile testing via Double Cantilever Beam specimens showed similar

results although with some cases having higher than expected variability. The cause of this variability remains to be determined.

The laser shockwave technique has been shown to be able to detect weak bonds between laminates. The developed technique is non-damaging if the bond is sufficiently strong for the shockwave loading applied. However, a correlation between the strength value measured by the technique at high strain rates and the strength measured by established quasi-static testing techniques (e.g. DCB) remains to be established.

In planned future work, since not all fabricated weak bond samples have been tested, NRC will continue laser shockwave testing on these to collect additional data.

5.0 ACKNOWLEDGEMENTS

The authors of this paper would like to acknowledge the dedicated work of Julieta Barroeta-Robles (Co-op Student, Carleton University) during the course of this work, as well as the support of the U.S. Army Research Laboratory for valuable help in consultation and with chemical tuning of the bond interfaces discussed here.

The work described in this paper was undertaken as part of a joint project with expert researchers from Laboratoire Procédés et Ingénierie en Mécanique et Matériaux (CNRS), Paris, France, and Département Physique et Mécanique des Matériaux, ENSMA, Cedex, France. The French researchers also performed laser shock testing on the controlled strength specimens described herein, and their excellent results are published in References [34] to [36]. Only the work performed by NRC Canada is described in this paper.

6.0 REFERENCES

[1] Davis, M., and Tomblin, J. "Best Practice in Adhesive-Bonded Structures and Repairs", DOT/FAA/AR-TN06/57 (2007), Based on presentation given at Federal Aviation Administration *Bonded Structures Workshop*, 2004.

[2] Orborne, J. H., Blohowiak, K.Y., and Sekits, D.F. "Environmentally Benign Sol-Gel Surface Treatment for Aluminum Bonding Applications." WL-TR-95-4060, *AFRL/MLSA*, 1996.

[3] Sacco, G.R, and Tanner, W.C. "Improved Adhesive Bond Permanence with Reactive Organosilane Coupling Agents." *Applied Sciences Division (DRDAR-LCA)*, 1978.

[4] Mazza, J.J. "Sol-Gel Technology For Low-Voc, Nonchromated Adhesive Bonding Application." AFRL-ML-WP-TR-2002-4131, *SERDP*, 2004.

[5] Jensen, R. E., and McKnight, S. H. "Novel Silane Based Fiber Sizings for Enhanced Energy Absorption." United States. Army Research Laboratory. *Proceedings of the 25th Annual Meeting of the Adhesion Society and the Second World Congress on Adhesion and Related Phenomena*, 2002.

[6] Barroeta-Robles, J., Cole, R., and Sands, J.M. "Development of Controlled Adhesive Bond Strength for Assessment by Advanced Non-Destructive Inspection Techniques", SAMPE Conference, Seattle, WA, USA, 2010.

[7] Barroeta-Robles, J., Cole, R., Sands, J.M., and Parker, T. "A Novel Approach to Generation of Adhesive Bonds with Controlled Bond Strength", American Society for Composites Conference, Dayton, OH, USA, 2010.

[8] R. L. Crane and G. Dillingham, "Composite bond inspection", J. Mater. Sci., Vol.43, pp. 6682-6694, 2008.

[9] I. J. Munns and G. A. Georgiou, "Non-destructive testing methods for adhesively bonded joint inspection: a review", Insight, Vol. 37, pp. 941-952, 1995.

[10] R. D. Adams and B.W. Drinkwater, "Non-destructive testing of adhesively-bonded joints", Int. J. Mater. Prod. Technol., Vol. 14, pp. 385-398, 1999.

[11] J. L. Vossen, "Adhesion measurement of thin films, thick films, and bulk coatings". ASTM Spec. Tech. Publ. Vol. 640, pp. 122-131, 1978.

[12] V. Gupta, A. S. Argon, J. A. Cornie and D. M. Parks, "Measurement of interface strength by laser-pulse-induced spallation", Mater. Sci. Eng., Vol. A126, pp. 105–117, 1990.

[13] J. Yuan, V. Gupta, "Measurement of interface strength by the modified laser spallation technique. I. Experiment and simulation of the spallation process", J. Appl. Phys., Vol. 74, pp. 2388-2397, 1993.

[14] V. Gupta , J. Yuan, "Measurement of interface strength by the modified laser spallation technique. II. Applications to metal/ceramic interfaces". J. Appl. Phys., Vol.74, pp. 2397-2404, 1993.

[15] A. Yu, V. Gupta, "Measurement of in situ fiber/matrix interface strength in graphite/epoxy composites", Comp. Sci. and Tech., Vol. 58, pp. 1827-1837, 1998.

[16] R. Bossi, K. House, C. T.Walters, D. Sokol, "Laser Bond Testing", Materials Evaluation, Vol. 67, pp. 819-827, 2009.

[17] M. Perton, A. Blouin and J.-P. Monchalin, "Adhesive bond testing of carbon-epoxy composites by laser shockwave", J. Phys. D: Appl. Phys., Vol. 44, 034012 (12 pp.), 2011.

[18] Morris, C.E.M "Strong, durable adhesive bonding: Some aspects of surface preparation, joint design and adhesive selection". *Materials Forum.* 17(1993): 211-218.

[19] Sacco, G.R and Tanner, W.C. "Improved Adhesive Bond Permanence with Reactive Organosilane Coupling Agents." *Applied Sciences Division (DRDAR-LCA).* NJ, USA, 1978.

[20] Mazza, J. J., Avram, J.B., and Kuhbander, R.J. "Grit-blast/silane (GBS) Aluminum Surface Preparation for Structural Adhesive Bonding." WL-TR-94-4111, *AFRL/MLSA*, OH, USA, 2003.

[21] Jensen, R.E and McKnight, S.H. "Inorganic-Organic Fiber Sizings for Enhanced Impact Energy Absorption in Glass Reinforced Composites", *Composites Science and Technology*, (2006): 66, 509.

[22] McKnight, S.H. *Private Communications* with author J.M. Sands. 10 Sep 2002 and 11 Jan 2010.

[23] Stewart, I., Chambers, A., and Gordon, T. "The cohesive mechanical properties of a toughened epoxy adhesive as a function of cure level". *International Journal of Adhesion & Adhesives*. Volume 27, Issue 4, pp. 277-287, 2007.

[24] *EA9394 Epoxy Paste Adhesive Data Sheet*. Henkel Corporation. Bay Point, CA, USA. 2002.

[25] "ASTM D 1002−05−Standard Test Method for Apparent Shear Strength of Single−Lap−Joint Adhesively Bonded Metal Specimens by Tension Loading (Metal−to−Metal)", *ASTM International*, West Conshohocken, PA., 2005.

[26] Morris, C.E.M "Strong, durable adhesive bonding: Some aspects of surface preparation, joint design and adhesive selection". *Materials Forum.* 17(1993): 211-218.

[27] *FM73 Toughened Epoxy Film Technical Data Sheet.* Cytec Engineered Materials Technical Service. Havre de Grace USA.

[28] "ASTM D5528-01(2007), Standard Test Method for Mode I Interlaminar Fracture Toughness of Unidirectional Fiber-Reinforced Polymer Matrix Composites.", *ASTM International*, West Conshohocken, PA., 2007.

[29] M. Perton, D. Levesque, J.-P. Monchalin, M. Lord, J. A. Smith and B. H. Rabin, "Laser shockwave technique for characterization of nuclear fuel plate interfaces", 39th Annual Review of Progress in QNDE, AIP Conf. Proc. 1511, pp. 345-352, 2013.

[30] R. Fabbro, J. Fournier, P. Ballard, D. Devaux and J. Virmont. "Physical study of laser-produced plasma in confined geometry", J. Appl. Phys., Vol. 68, pp. 775–781, 1990.

[31] L. M. Barker, "The development of the VISAR and its use in shock compression science", in Shock Compression of Condensed Matter., edited by M. D. Furnish, L. C. Chhabildas, and R. S. Hixson, (Melville New York), pp. 11-17, 1999.

[32] M. Arrigoni, J.-P. Monchalin, A. Blouin, S.E. Kruger and M. Lord, "Laser Doppler interferometer based on a solid Fabry–Perot etalon for measurement of surface velocity in shock experiments", Meas. Sci. Technol. Vol. 20, 015302 (7pp), 2009.

[33] J.-P. Monchalin "Laser-ultrasonics: principles and Industrial Applications", Chapter 4, in "Ultrasonic and Advanced Methods for Nondestructive Testing and Material Characterization", C.H. Chen ed., World Scientific Publishing Co., pp. 79-115, 2007.

[34] M. Boustie, E. Gay, L. Berthe, M. Arrigoni, J. Radhakrishnan, T. de Résséguier, M. Perton, A. Blouin, and J.P. Monchalin, "Laser Shock Adhesion Test (LASAT) of composite materials for aerospace industry", Surface Modification Technologies Conference (SMT23), Mamallapuram, Chennai(Madras), India, 2009.

[35] E. Gay, L. Berthe, M. Boustie, M. Arrigoni, A. Johnston, R. Cole, J. Barroeta, and E. Buzaud, "Experimental and Numerical Investigation of Composite Behaviour at High Strain Rate", 19th DYMAT Technical Meeting, Strasbourg, France, 2010.

[36] E. Gay, L. Berthe, M. Boustie, M. Arrigoni, A. Johnston, R. Cole, J. Barroeta, and E. Buzaud, "Experimental investigation of a composite behaviour under ultra-short laser-shock loading", Surface Modification Technologies Conference (SMT24), Dresden, Germany, 2010.